Frontiers in Computing and Intelligent Systems
ISSN: 2832-6024 | Vol. 14, No. 3, 2025

Analysis of Abnormal Brain Networks in Autism Based on fMRI

Yuxin Chang [1], Yuansha Xie [1], Qi Mao [1], Jing Luo [2], Cheng Ju [1,*], Weiwei Xue [1] and Wenyao Yan [1]

[1] School of Data Science and Engineering, Xi'an Innovation College of Yan'an University, Xi'an, Shaanxi, China
[2] School of Computer Science and Engineering, Xi'an University of Technology, Xi'an, Shaanxi, China

*** Corresponding author:** Cheng Ju

Abstract: Autism spectrum disorder (ASD) is characterized by widespread neurodevelopmental impairments, with emotional and behavioral deficits linked to abnormal local brain function and functional connectivity. Investigating whether the intrinsic functional brain network topology in ASD is altered is therefore of critical diagnostic importance. To identify aberrant brain networks in ASD, this study constructed functional networks based on 90 brain regions defined by an automated anatomical atlas, followed by network-based statistics (NBS) and graph-theoretical analyses. The findings were further validated using support vector machine (SVM) classification between ASD and neurotypical participants. NBS revealed that abnormalities in functional connectivity in ASD were predominantly located within the default mode and sensorimotor networks, involving regions in the temporal and frontal lobes, basal ganglia, and parts of the limbic system. Graph-theoretical analysis further indicated that topological alterations in ASD likely stem from dysregulated connectivity within these subnetworks, demonstrating significantly impaired efficiency in both information transfer and integration compared to controls—a finding potentially linked to characteristic ASD behavioral profiles. Using these aberrant connections as biological features, a systematic evaluation of multiple classifiers identified SVM as optimal. Through cross-validation and parameter tuning, classification achieved an accuracy of 84.86% on the NYU dataset. To further validate the generalizability of the identified network features, corresponding functional connections were extracted from the larger UM dataset (sample size >80), yielding a classification accuracy of 72.64%, confirming the clinical relevance of the detected network abnormalities. These results highlight abnormal topological organization in functional brain networks in ASD and provide novel insights into the neural mechanisms underlying communication deficits and repetitive behaviors in autism.

Keywords: Autism Spectrum Disorder; Functional Brain Networks; Network Analysis; Graph-theoretical Analysis; Topological Structure.

1. Introduction

Autism Spectrum Disorder (ASD) is a heterogeneous and evolving neurodevelopmental condition. Individuals with ASD are characterized by a triad of core deficits in social interaction, verbal and non-verbal communication, and imagination, alongside restricted, repetitive patterns of behavior and interests [1]. Although the precise onset of symptoms varies considerably among individuals, a preponderance of clinical evidence indicates a high prevalence in early childhood, with symptoms typically persisting throughout the lifespan. These symptoms primarily manifest as impairments in social communication, diminished capacity for reciprocal interaction, reduced interest in social stimuli, limited emotional expression, and the presence of stereotyped behaviors [2].

Reported prevalence rates underscore ASD as a significant global public health concern. Worldwide, it is estimated to affect over 67 million individuals. Notably, the estimated prevalence among children has risen from 1 in 88 in 2009 to approximately 1 in 45 in recent years. In China, data from the China Disabled Persons' Federation indicate an ASD prevalence of 0.7%, affecting more than 10 million individuals, with an annual growth rate of about 10%, including an estimated 2 million children under the age of 12. ASD profoundly impacts daily living, communication, and learning, posing substantial long-term challenges to the psychological and physical well-being of affected individuals. Despite remarkable advances in other medical fields, ASD research faces a distinct and persistent challenge: the absence of objective biological markers. Consequently, elucidating the etiology and underlying neurobiological mechanisms of ASD remains a paramount and unresolved puzzle for the global medical community. Initiatives such as the 2013 campaign by the Centers for Disease Control and Prevention aimed to raise public awareness of ASD and related developmental delays [3]. This growing awareness has fueled support for early intervention and stimulated extensive research into early diagnosis and treatment strategies.

In line with this imperative, the American Academy of Pediatrics (AAP) recommends standardized screening for ASD during early social development to facilitate timely intervention, access to support services, and improved long-term outcomes [4, 5]. Research in pediatric settings has demonstrated the superior effectiveness of combined developmental surveillance and standardized screening tools over either approach alone for accurately identifying social delays and ASD risk [6]. Children who receive both monitoring and screening are significantly more likely to be enrolled in early intervention services [7]. Thus, early screening and identification are critical for initiating appropriate support, enhancing quality of life, and laying a stronger foundation for future development.

However, a critical gap persists in current diagnostic paradigms. In practice, the diagnosis of ASD continues to rely heavily on the observation of behavioral symptoms and the application of assessment scales, a process that necessitates detailed clinical interviews and comprehensive

developmental history-taking. While behavioral phenotyping is invaluable, its true potential is unlocked only when it enables the quantification of relationships between observable symptoms and their latent neurobiological substrates[8]. The prevailing global reliance on clinical observation for ASD diagnosis presents inherent limitations: it is inherently time-consuming, complex, and susceptible to subjective interpretation[9]. Therefore, the pursuit of objective biological markers is not merely supplementary but essential for a more profound and mechanistic understanding of the disorder.

To address these limitations, this study investigates the intrinsic functional brain networks in ASD using resting-state functional magnetic resonance imaging (fMRI) data. We employ network-based statistics and graph-theoretical analyses to identify and characterize significant alterations in the functional connectome of individuals with ASD compared to neurotypical controls. Subsequently, the discriminative power of these identified network abnormalities is rigorously validated by applying machine learning classification. The results not only confirm the efficacy of our network-based approach for ASD classification but also provide crucial insights into the aberrant neural circuitry that may underlie the pathogenesis of ASD, thereby contributing to the foundational search for its objective neurobiological signatures.

2. Methods

The fMRI-based analysis of abnormal brain networks in Autism Spectrum Disorder (ASD) consisted of four main stages: (1) data preprocessing, (2) functional brain network construction, (3) network-based and graph-theoretical analyses, and (4) classification validation. An overview of the workflow is presented in Fig. 1.

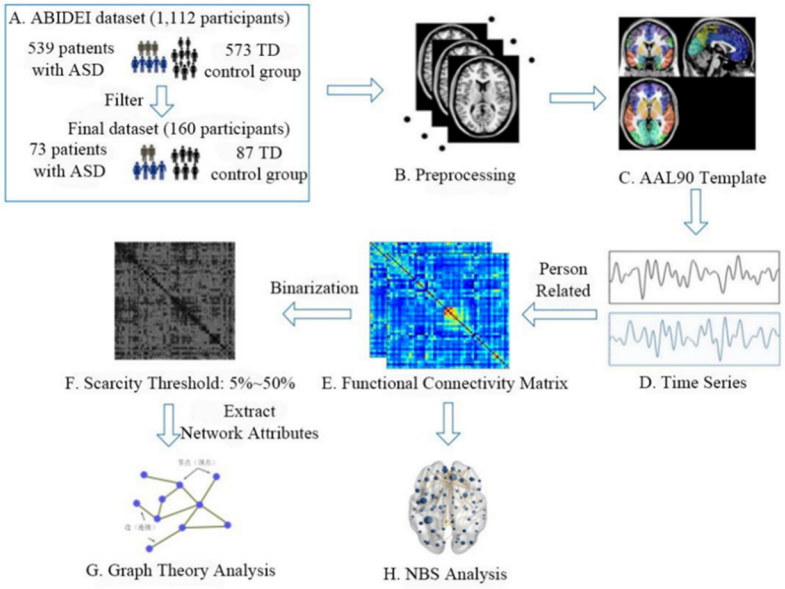

Fig 1. Flowchart for researching NBS and topological properties of ASD

2.1. Dataset and Data Preprocessing

Experimental data were obtained from the Autism Brain Imaging Data Exchange repository [3]. To mitigate site-specific variability and ensure a robust sample size, data from the New York University (NYU) site were selected, comprising resting-state fMRI scans from 74 individuals with ASD and 98 typically developing (TD) controls.

To control for the potential confounding effects of significant group differences in sex and to reduce false positive rates induced by excessive head motion [10], data were rigorously screened. Subjects with head motion exceeding 2° of rotation or 2 mm of translation were excluded. Following this procedure, data from 1 ASD and 11 TD subjects were removed. The final dataset included 73 ASD and 87 TD subjects. Subsequent analysis confirmed no significant between-group differences in age ($p = 0.9620$) or sex ($p = 0.1853$). Demographics of the final sample are summarized in Table 1.

Table 1. Data of ASD patients and TD participants.

	ASD	TD	Value of p
Sample Size	73	87	--
Number of genders (Male: Female)	63:10	68:19	0.1853
Year	14.71±7.16	14.76±5.45	0.9620

All fMRI data were preprocessed using the DPARSF toolbox (V5.3, http://www.rfmri.org) [11], based on SPM12. The standard preprocessing pipeline included: (1) format conversion to NIFTI; (2) removal of the first 10 time points to allow for signal stabilization; (3) slice timing correction; (4) head motion correction (subjects with motion >2 mm or 2°

were excluded); (5) spatial normalization to the Montreal Neurological Institute (MNI) template at a resolution of 3×3×3 mm³, co-registration with individual T1-weighted images, segmentation into gray matter, white matter, and cerebrospinal fluid, and nuisance signal regression (Friston's 24 motion parameters, linear drift, and signals from white matter and cerebrospinal fluid); (6) spatial smoothing with an 8 mm full-width at half-maximum Gaussian kernel; (7) linear detrending; and (8) band-pass temporal filtering (0.01–0.08 Hz).

2.2. Functional Brain Network Construction

For each participant, a functional brain network was constructed. The network nodes were defined by the 90 cortical and subcortical regions of interest (ROIs) from the Automated Anatomical Labeling (AAL) atlas [12] (Fig. 2). The mean time series was extracted from each ROI. A 90×90 functional connectivity (FC) matrix was generated for each subject by computing the Pearson correlation coefficient between the time series of every pair of ROIs. The resultant correlation coefficients were subsequently transformed to z-scores using Fisher's r-to-z transformation to improve normality.

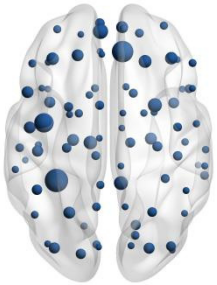

Fig 2. The position of the AAL90 node

2.3. Network-based Statistics (NBS)

NBS is a non-parametric method with family-wise error (FWE) correction for multiple comparisons, designed to identify connected components of links that differ significantly between groups [13]. Using the NBS toolbox (https://www.nitrc.org/projects/nbs), we assessed significant differences in functional connectivity components between the ASD and TD groups, testing separately for both hyperconnectivity (ASD > TD) and hypoconnectivity (ASD < TD).

The NBS procedure was implemented in three steps: First, an independent two-sample t-test was performed for each connection in the FC matrices. All connections with a t-statistic exceeding a primary, uncorrected threshold of $p < 0.001$ were retained. Second, among these suprathreshold connections, connected components (clusters) were identified based on their topological adjacency. Finally, for each identified component, a corrected p-value was calculated using a non-parametric permutation test (5000 permutations). A component was considered statistically significant if its FWE-corrected p-value was below 0.05.

2.4. Graph-theoretical Network Analysis

Graph theory was employed to characterize the topological organization of the functional brain networks. The binary, undirected adjacency matrices for analysis were derived by applying a proportional sparsity threshold to the individual z-transformed FC matrices. Connections with the top n% of weights were retained (value=1), while others were set to zero (value=0). The sparsity threshold (n) was varied from 5% to 50% in 1% increments. A minimum threshold of 5% was chosen to ensure network connectedness without isolated nodes. For each resulting binary network across this sparsity range, a set of global and local graph metrics was computed using the GRETNA toolbox (V2.0, http://www.nitrc. org/ projects/ gretna/) [14].

Global metrics included: global efficiency (Eglob), local efficiency (Eloc), clustering coefficient (Cp), characteristic path length (Lp), modularity (Q), and small-world properties (normalized clustering coefficient γ, normalized path length λ, and small-worldness σ). Eglob quantifies the efficiency of parallel information transfer across the entire network. Eloc reflects the fault tolerance of the network, indicating communication efficiency among a node's immediate neighbors if that node is removed. Cp measures the extent of local clustering or cliquishness. Lp quantifies the average shortest path length between any two nodes, indicating routing efficiency. Q measures the strength of division of the network into modules. Small-world properties indicate an optimal balance between network integration (low Lp) and segregation (high Cp).

Local (nodal) metrics included: nodal degree (Dnodal), nodal efficiency (Enodal), and nodal participation coefficient (PCnodal). Dnodal reflects the number of direct connections a node has. Enodal measures the efficiency of parallel information transfer from a given node to all others. PCnodal quantifies how well a node connects across different modules, indicating its role in inter-modular integration.

To integrate the topological information across the sparsity range, the area under the curve (AUC) was calculated for each graph metric (for each node in the case of local metrics) as a scalar, threshold-independent summary measure. Statistical group comparisons of these AUC values were performed using IBM SPSS Statistics. Visualization of network results was performed using the BrainNet Viewer toolbox (https://www.nitrc.org/projects/bnv/) [6].

3. Discussion

3.1. Altered Functional Connectivity in ASD

To characterize functional connectivity (FC) alterations between individuals with ASD and TD controls, subject-specific connectivity matrices (90×90) were generated by calculating Pearson correlation coefficients between the BOLD time series of each pair of nodes defined by the AAL90 atlas. These values, ranging between -1 and 1, were subsequently Fisher z-transformed to approximate normality for group-level analysis. The group-averaged FC matrices for both ASD and TD groups are visualized in Fig. 3. The left panel displays the whole-brain average functional connectivity matrix for the ASD group based on the AAL90 atlas template, while the right panel shows the corresponding matrix for the TD group. The color scale represents the strength of functional interaction between any two brain regions. The symmetric nature of the matrices is evident, with the diagonal representing self-correlation (which was excluded from subsequent analyses along with one half of the symmetric matrix). Visual inspection suggests broad patterns of both increased and decreased inter-regional coupling in ASD, motivating a more targeted, network-based statistical approach.

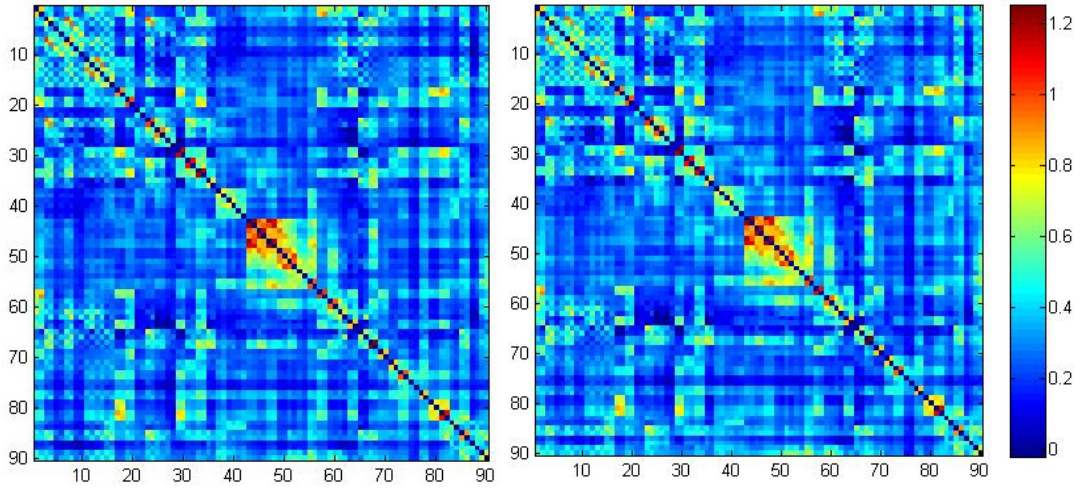

Fig 3. Visualization of FC matrices for ASD and TD

3.2. Identification of Disrupted Subnetworks via NBS

Network-Based Statistics (NBS) was employed to identify interconnected components of links showing significant between-group differences, controlling for family-wise error. Our analysis revealed a significant hyperconnected subnetwork in the ASD group compared to TD controls (FWE-corrected $p < 0.05$). This aberrant subnetwork primarily involved regions within the default mode network (DMN) and the sensorimotor network, including the dorsomedial prefrontal cortex, medial prefrontal cortex, anterior cingulate cortex, and hippocampus. Extensions into the visual network were also observed, encompassing the right cuneus, left superior and middle occipital gyri, and left fusiform gyrus (Fig. 4). This pattern of hyperconnectivity, particularly within and between the DMN—a network central to self-referential thought and social cognition—and sensorimotor regions, aligns with the "over-connectivity" hypothesis in ASD. It may reflect impaired pruning or atypical functional specialization, potentially underlying difficulties in shifting attention between internal and external stimuli and contributing to core social and sensory processing symptoms.

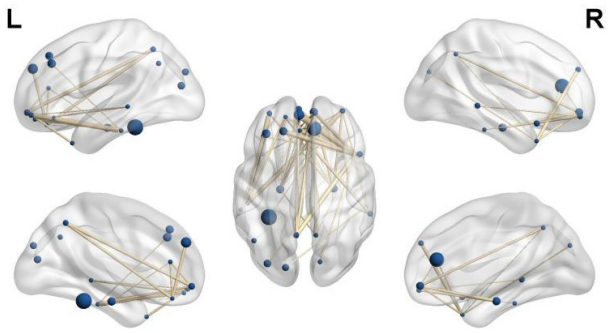

Fig 4. Abnormal regions and connectivity after NBS analysis between ASD and TD

3.3. Altered Topological Organization of Brain Networks

Table 2. The alterations of global network properties in ASD compared to TD group

	ASD	TD	Vaule of t	Vaule of p
Eglob	0.315	0.302	2.403	0.017*
Eloc	0.392	0.364	0.234	0.815
Cp	0.264	0.265	-1.376	0.204
Lp	3.215	3.363	2.230	0.027*
γ	0.829	0.817	0.641	0.521
λ	0.489	0.490	-0.379	0.658
σ	0.741	0.730	0.679	0.498

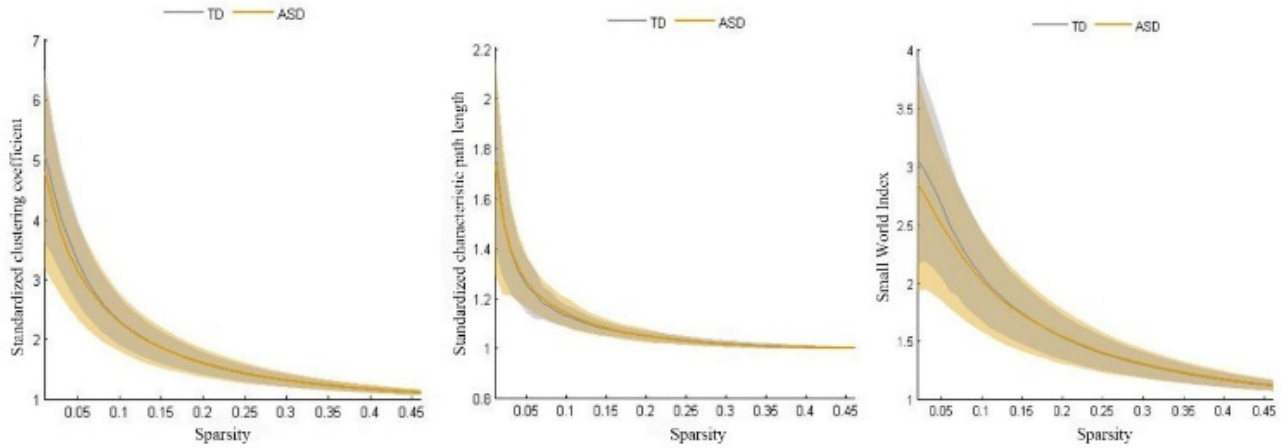

Fig 5. Curve of small-world properties parameters as a function of threshold variation

Graph-theoretical analysis across a range of sparsity thresholds confirmed that both ASD and TD groups exhibited small-world architecture (normalized $\gamma >> 1$, $\lambda >> 1$, $\sigma \approx 1$), indicative of an efficient balance between local segregation and global integration. However, significant between-group differences emerged in key global metrics. Specifically, the ASD group demonstrated a significantly lower Area Under the Curve (AUC) for characteristic path length (Lp, $p < 0.05$) and a significantly higher AUC for global efficiency (Eglob, $p < 0.05$) compared to the TD group (Table 2, Fig. 5).

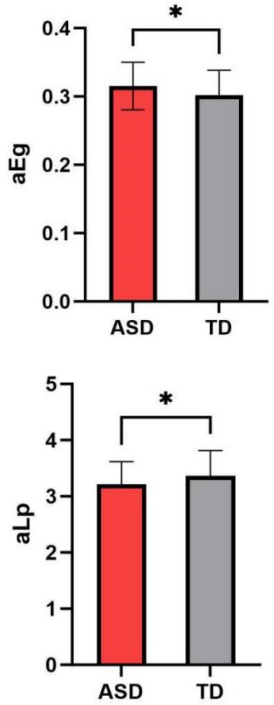

Fig 6. The ASD group exhibits significantly different global indicators

This finding signifies a shift in the ASD functional connectome toward a more randomized or less optimized topological configuration. Shorter Lp and higher Eglob suggest an enhanced potential for global information transfer. While this may superficially appear advantageous, in the context of neurodevelopmental disorders like ASD, it is often interpreted as a loss of optimal network differentiation—a potential hallmark of "neural noise" or reduced functional segregation. Our study localizes these topological shifts to specific dysfunctional subnetworks identified by NBS, providing a more nuanced link between localized connectional abnormalities and global network reorganization.

3.4. Validation through Machine Learning Classification

To evaluate the clinical translational potential of the identified network abnormalities, we employed them as features for machine learning classification analysis. The classification performance was comprehensively assessed using five metrics: accuracy, sensitivity, specificity, positive predictive value (PPV), and negative predictive value (NPV). Accuracy reflects the overall prediction precision; sensitivity represents the proportion of true ASD samples correctly identified; specificity indicates the proportion of true TD samples correctly excluded. Classification performance was quantified using four fundamental metrics from the confusion matrix: true positive (TP), false negative (FN), true negative (TN), and false positive (FP). Specifically, TP denotes correctly classified true ASD samples; FN indicates true ASD samples misclassified as TD; TN refers to correctly classified true TD samples; FP represents true TD samples misclassified as ASD.

The formulas for each metric are as follows:

$$Accuracy\ Rate = \frac{TP + TN}{TP + TN + FP + FN} \times 100\% \quad (1)$$

$$Sensitivity = \frac{TP}{TP + FN} \times 100\% \quad (2)$$

$$Specificity = \frac{TN}{TN + FP} \times 100\% \quad (3)$$

$$PPV = \frac{TP}{TP + FP} \times 100\% \quad (4)$$

$$NPV = \frac{TN}{TN + FN} \times 100\% \quad (5)$$

Through the systematic evaluation of these metrics, the discriminative efficacy of the classifier for ASD versus TD can be comprehensively quantified, providing a quantitative basis for clinical auxiliary diagnosis. The translational potential of the identified network anomalies was evaluated

by employing them as features for machine learning classification. A systematic comparison of five classifiers using 10-fold cross-validation on the NYU dataset identified Support Vector Machine (SVM) as the best performer, achieving an accuracy of 84.86%, with balanced sensitivity and specificity (Table 3).

Table 3. Calculation results of different classifiers

	Naive Bayes	AdaBoost	**SVM**	Random Forest	KNN
ACC	80.00%	68.57%	**84.86%**	77.14%	71.43%
SEN	86.36%	72.73%	**95.45%**	86.36%	86.36%
SPE	69.23%	61.54%	61.54%	61.54%	46.15%
PPV	82.61%	76.19%	80.77%	79.17%	73.08%
NPV	75.00%	57.14%	**88.89%**	72.73%	66.67%
F1	84.44%	74.42%	**87.50%**	82.61%	79.17%

Further optimization of the SVM via k-fold cross-validation (k=5, 10, 20) confirmed that 10-fold validation yielded the most robust performance (Table 4). This high classification accuracy on the primary dataset strongly suggests that the network features derived from our NBS and graph-theory analyses capture biologically meaningful distinctions between ASD and TD brain states.

Table 4. Classification results of cross-validation on the NYU dataset

	5-fold CV	**10-fold CV**	20-fold CV
ACC	80.00%	**84.86%**	77.58%
SEN	86.36%	**95.45%**	84.36%
SPE	69.23%	61.54%	65.24%
PPV	82.61%	80.77%	78.15%
NPV	84.44%	**88.89%**	84.61%

To test the generalizability of these features as potential biomarkers, we applied the same pipeline—extracting FC values from the identical connections identified as significant in the NYU NBS analysis—to an independent sample from the University of Michigan (UM) site within ABIDE (n > 80). The classification accuracy on this held-out dataset was 72.64% (Table 5). While slightly lower, likely due to cross-site variability in acquisition protocols and participant characteristics, this result remains significantly above chance and provides critical external validation. It supports the notion that the discovered aberrant subnetwork possesses reproducible, site-invariant discriminatory power, reinforcing its candidacy as a network-level neurobiological signature of ASD.

Table 5. Classification results of cross-validation on the UM dataset

	5-fold CV	**10-fold CV**	20-fold CV
ACC	70.00%	**72.64%**	70.58%
SEN	76.36%	**85.32%**	81.36%
SPE	69.23%	69.13%	68.24%
PPV	72.61%	71.51%	74.15%
NPV	64.44%	**68.74%**	62.61%

4. Conclusion

Autism Spectrum Disorder (ASD) imposes profound and often irreversible neurological challenges on patients' daily functioning, learning, and social interactions, resulting in significant long-term burdens for families and society. This underscores the urgent need for early diagnosis and intervention. Currently, ASD diagnosis relies heavily on subjective observational scales based on parental reports and clinical assessments. In this study, we identified distinct abnormal brain networks that differentiate ASD from neurotypical development, offering a promising objective approach to augment clinical diagnostics. Using network-based statistics (NBS), we found that individuals with ASD exhibit aberrant functional connectivity primarily within the default mode and sensorimotor networks, involving the temporal and frontal lobes, limbic system, basal ganglia, and extending to visual regions such as the left middle occipital gyrus and fusiform gyrus, with these alterations being interrelated rather than isolated. Graph-theoretical analysis further revealed that, although both ASD and typically developing groups show small-world organization, ASD networks display significant topological disturbances, including reduced nodal efficiency in the left globus pallidus and thalamus. These findings suggest that the functional connectivity abnormalities identified via NBS may stem from underlying topological disruptions in the ASD connectome. By leveraging these aberrant subnetworks as discriminative features in a machine learning framework, support vector machine (SVM) achieved 84.86% classification accuracy on the NYU dataset through cross-validation. Generalizability was confirmed on an independent UM dataset, with an accuracy of 72.64%, reinforcing the neurobiological relevance of dysregulated connectivity in key regions such as the dorsomedial and medial prefrontal cortex, anterior cingulate cortex, and hippocampus. In summary, this study integrates NBS and graph-theoretical analyses to identify a reproducible aberrant functional subnetwork in ASD, demonstrating its potential as a diagnostic biomarker and providing mechanistic insights into ASD neuropathology. Future research should explore links between resting-state abnormalities and task-evoked neural dynamics, employ longitudinal designs to track neural changes, and consider age and sex stratification to advance personalized intervention strategies for ASD.

Acknowledgments

This paper was supported by the "Humanoid Robot + Curriculum" Teaching Reform Research Special Project of Xi'an Innovation College of Yan'an University(2024YKG15) and the Scientific Research Projects of Xi'an Innovation College of Yan'an University(2025XJKY09).

References

[1] Wing L. The autistic spectrum. 1997, 350: 1761-1766.

[2] Segal D L. Diagnostic and Statistical Manual of Mental Disorders (DSM-IV-TR). The Corsini Encyclopedia of Psychology. 1-3.

[3] Daniel K L, Prue C, Taylor M K, et al. 'Learn the signs. Act early': a campaign to help every child reach his or her full potential. Public health, 2009, 123 Suppl 1: 11-16.

[4] Briggs R D, Stettler E M, Silver E J, et al. Social-emotional screening for infants and toddlers in primary care. Pediatrics, 2012, 129(2): 377-384.

[5] Weitzman C, Wegner L. Promoting optimal development: screening for behavioral and emotional problems. Pediatrics, 2015, 135(2): 384-395.

[6] Gabrielsen T P, Farley M, Speer L, et al. Identifying autism in a brief observation. Pediatrics, 2015, 135(2): 330-338.

[7] Barger B, Rice C, Wolf R, et al. Better together: Developmental screening and monitoring best identify children who need early intervention. Disability and health journal, 2018, 11(3): 420-426.

[8] Lee H, Marvin A R, Watson T, et al. Accuracy of phenotyping of autistic children based on Internet implemented parent report. American journal of medical genetics Part B, Neuropsychiatric genetics: the official publication of the International Society of Psychiatric Genetics, 2010, 153b (6): 1119-1126.

[9] Nagai Y, Kirino E, Tanaka S, et al. Functional connectivity in autism spectrum disorder evaluated using rs-fMRI and DKI. CEREBRAL CORTEX, 2023.

[10] Yan C G, Cheung B, Kelly C, et al. A comprehensive assessment of regional variation in the impact of head micromovements on functional connectomics. NeuroImage, 2013, 76: 183-201.

[11] Dawson G, Rogers S, Munson J, et al. Randomized, controlled trial of an intervention for toddlers with autism: the Early Start Denver Model. Pediatrics, 2010, 125(1): 17-23.

[12] Tzourio-Mazoyer N, Landeau B, Papathanassiou D, et al. Automated anatomical labeling of activations in SPM using a macroscopic anatomical parcellation of the MNI MRI single-subject brain. NeuroImage, 2002, 15(1): 273-289.

[13] Zalesky A, Fornito A, Bullmore E T. Network-based statistic: identifying differences in brain networks. NeuroImage, 2010, 53(4): 1197-1207.

[14] Pinto-Martin J A, Young L M, Mandell D S, et al. Screening strategies for autism spectrum disorders in pediatric primary care. Journal of developmental and behavioral pediatrics: JDBP, 2008, 29(5): 345-350.